

states of aryl radicals were formed in fragmentation step 2, in proportions depending on the identity of X, and that one type of state yielded ultimately arylacetone and the other type 1-aryl-2-propanol. Both these models were dismissed for reasons that will be argued in later full publication.

One model of reaction during mixing fails to accommodate the data. According to it, an electron-rich zone of solution, which may contain enolate ions but no aryl halide molecules, advances smoothly in the manner of a phalanx into an "electronless" zone containing both aryl halide and enolate species. A particular aryl halide molecule is suddenly surrounded by solvated electrons, and thereafter it and any species derived from it exist in an electron-rich environment. On this model, PhI and PhCl should give identical product proportions, and indeed both would give mainly benzene inasmuch as the aryl radical should react faster with the solvated electron (step 6) than with the enolate ion (step 3) when both are present in substantial concentration.

A second mixing model provides useful insight. It is one of ragged advance, in which raiding parties of solvated electrons sortie into the "electronless" zone and are annihilated upon encountering aryl halide molecules (step 1). The resulting  $[\text{ArX}]^-$ 's, being momentarily in an "electronless" zone, have an opportunity to undergo the sequence of steps 2-5 to form the enolate ion of the arylacetone product.<sup>5</sup> Fragmentation step 2 is much faster for  $[\text{ArI}]^-$  than for the corresponding  $[\text{ArCl}]^-$ ,<sup>6</sup> and therefore the several intermediates derived from ArI have a better chance of completing steps 2-5 before the main force of solvated electrons arrives. When the main force arrives, steps 6 and 8 rapidly occur and dominate product formation. One thus interprets a strong leaving group effect on product composition in terms of a *microscopic* effect, namely, competition between rate of electron advance and rate of fragmentation of  $[\text{ArX}]^-$ , the latter known to depend on the identity of X.<sup>7</sup>

However, this model gives no interpretation of why an aryl chloride serves to increase the ketone/alcohol product ratio from an aryl iodide also present. We suggest that ArCl-derived intermediates (aryl radicals and radical anions of type 3), which remain after most of the corresponding ArI-derived species have reacted, may combine sacrificially with an ensuing surge of solvated electrons so as to protect the ArI-derived intermediates from assault. This could happen only if the two series of reacting intermediates were spatially separated, with the ArCl-derived species closer to the front of advancing solvated electrons and the ArI-derived species deeper within the "electronless" zone. That state of affairs might develop if at least part of the electron advance were by tunneling, and if electrons could tunnel farther to get to ArI molecules than to aryl radicals or radical anions of type 3. In that case electrons could tunnel through a thin reaction zone, populated largely by ArCl-derived intermediates, to ArI molecules farther from the front where the latter could then react behind a protective screen of ArCl-derived intermediates.

Much of the migration of solvated electrons is believed to occur by tunneling,<sup>10</sup> and there is evidence that electrons can tunnel farther to PhI than to PhCl molecules.<sup>11-13</sup> Plausibly their ability to tunnel to Ar- or 3 species is limited to even shorter distances.

Clearly both the experimental phenomenon that we describe and the interpretations that we offer call for further attention. Nevertheless, it is evident that, when reaction occurs during mixing, the product formed from a reactive intermediate may depend not only on what it is, but on where and when it is formed.

**Acknowledgment.** This research was supported in part by the National Science Foundation and in part by the Petroleum Research Fund, administered by the American Chemical Society.

## References and Notes

- (1) Rossi, R. A.; Bunnett, J. F. *J. Am. Chem. Soc.* **1972**, *94*, 683.
- (2) Bunnett, J. F. *Acc. Chem. Res.* **1978**, *11*, 413.
- (3) Anbar, M.; Hart, E. J. *J. Am. Chem. Soc.* **1964**, *86*, 5633.
- (4) Boyle, W. J., Jr.; Bunnett, J. F. *J. Am. Chem. Soc.* **1974**, *96*, 1418.
- (5) We have shown experimentally that the enolate ion of 1 is little affected by excess solvated electrons.
- (6) Alwair, K.; Grimshaw, J. J. *Chem. Soc., Perkin Trans. 2* **1973**, 1811. Nelson, R. F.; Carpenter, A. K.; Seo, E. T. *J. Electrochem. Soc.* **1973**, *120*, 206. See also: Saveant, J.-M.; Thiebaut, A. *J. Electroanal. Chem.* **1978**, *89*, 335. Amatore, C.; Chaussard, J.; Pinson, J.; Saveant, J.-M.; Thiebaut, A. *J. Am. Chem. Soc.* **1979**, *101*, 6012.
- (7) If fragmentation of  $[\text{ArX}]^-$  were very slow, it might be surrounded by solvated electrons before it fragmented. In that case steps 6 and 7 forming benzene or derivative thereof may well predominate, and no arylacetone or 1-aryl-2-propanol may be formed.<sup>8</sup> This constitutes an alternative interpretation for an earlier observation<sup>9</sup> that, whereas many PhX's react with acetone enolate ion and potassium according to eq P1, others are cleaved to form benzene without 1 or 2.
- (8) Cf. Bunnett, J. F.; Gloor, B. F. *Heterocycles* **1976**, *5*, 377.
- (9) Rossi, R. A.; Bunnett, J. F. *J. Am. Chem. Soc.* **1974**, *96*, 112.
- (10) Pilling, M. J.; Rice, S. A. *J. Chem. Soc., Faraday Trans. 2* **1975**, 1563; *J. Phys. Chem.* **1975**, *79*, 3035.
- (11) Namiki, A.; Noda, M.; Higashimura, T. *J. Phys. Chem.* **1975**, *79*, 2975; *Bull. Chem. Soc. Jpn.* **1975**, *48*, 3073. Shimokawa, T.; Sawai, T. *Ibid.* **1977**, *50*, 365.
- (12) In separate reactions, deeper tunneling to PhI than to PhCl would also contribute to enhancement of the 1/2 ratio from PhI over PhCl.
- (13) The concept of electron transfer at a greater distance to iodine than to chlorine compounds provides an alternative interpretation for the fact<sup>14</sup> that in reactions of alkyl halides with disodium tetraphenylethylene the yields of reduction products (as contrasted to products of alkylation of tetraphenylethylene) decrease in the order RI > RBr > RCl. On this concept, the alkyl radical formed immediately after electron transfer to an alkyl iodide, compared with an alkyl bromide or chloride, is farther from the by-product tetraphenylethylene radical anion and, so to speak, has a head start on getting away from it.
- (14) Garst, J. F.; Roberts, R. D.; Pacifici, J. A. *J. Am. Chem. Soc.* **1977**, *99*, 3528.

Raymond R. Bard, J. F. Bunnett\*  
Xavier Creary, Michael J. Tremelling

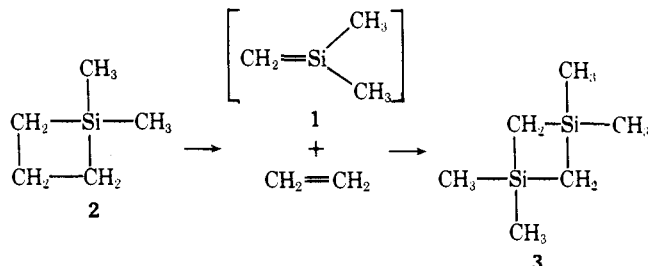
University of California, Santa Cruz, California 95064

Received August 20, 1979

## An Electron Diffraction Study of 1,1-Dimethylsilaethylene

Sir:

Although attempts to synthesize stable molecules containing carbon-silicon double bonds date back to nearly the turn of the century,<sup>1</sup> all efforts have been unsuccessful. In 1966 Gusel'nikov provided a number of lines of indirect evidence that 1,1-dimethylsilaethylene (DMSE, **1**) is a short-lived intermediate in the thermolysis of 1,1-dimethylsilacyclobutane (DMSCB, **2**), yielding 1,1,3,3-tetramethyl-1,3-disilacyclobutane (TMDSCB, **3**) and ethylene.<sup>1,2</sup> Subsequently, inter-



mediates possessing carbon-silicon double bonds have been postulated in a variety of retrocycloadditions, thermal and photochemical rearrangements, and elimination reactions.<sup>1</sup> Theoretical discussions of the structure, stability, and lack of persistence of silaalkenes abound.<sup>3</sup> Several spectroscopic investigations of silaalkenes have been published.<sup>4,5</sup> We report herein the first structural study of a molecule containing a carbon-silicon double bond, a gas-phase electron diffraction study of DMSE (**1**).

DMSE was generated by the pyrolysis of DMSCB. Gen-

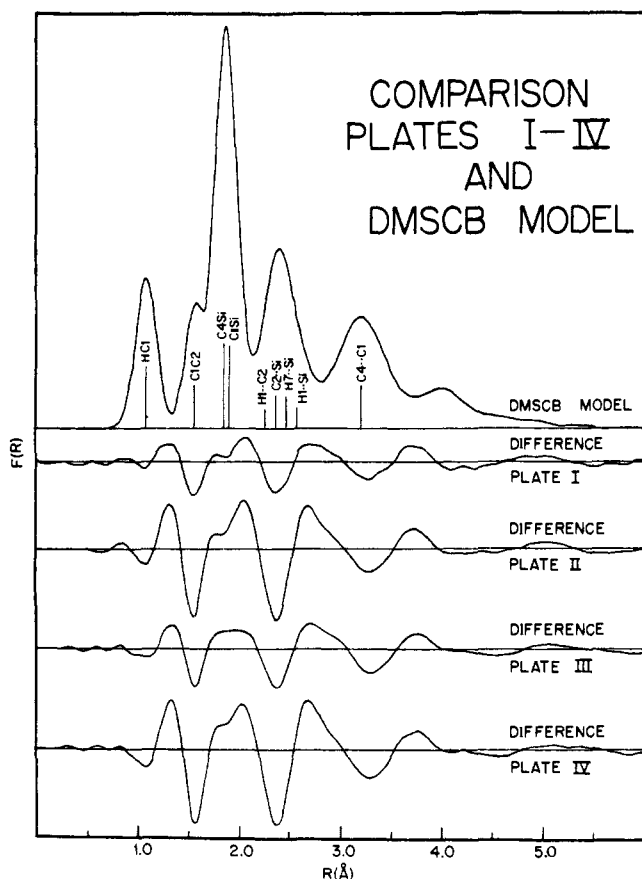
**Table I.** Products of Plates I-IV

plate	nozzle, ga	$T_t$ , °C <sup>b</sup>	$T_a$ , °C <sup>c</sup>	products, % <sup>a</sup>				res <sup>d</sup>	$R^e$
				DMSCB	DMSE	TMDSCB	CH <sub>2</sub> =CH <sub>2</sub>		
I	20	970	750	60 (11)	23 (8)	10 (19)	8 (6)	0.78	0.09
II	20	1070	780	22 (9)	35 (6)	17 (14)	26 (4)	0.96	0.14
III	16	1070	820	52 (8)	26 (6)	9 (14)	13 (4)	0.87	0.10
IV	16	1180	870	12 (5)	49 (4)	18 (9)	21 (3)	0.95	0.09

<sup>a</sup> Error limits in parentheses are three times the standard deviations. <sup>b</sup> Thermocouple temperature at nozzle tip. <sup>c</sup> Average pyrolysis temperature as estimated from extent of DMSCB decomposition. <sup>d</sup> Index of resolution. <sup>e</sup> Intensity  $R$  factor,  $R = (\sum \omega_i (I_{\text{obsd}} - I_{\text{calcd}})^2 / \sum \omega_i I_{\text{obsd}}^2)^{1/2}$ .

eration took place in a high temperature nozzle system that was developed for the study of *p*-xylylene.<sup>6</sup> The electron diffraction data were recorded at the Indiana University Molecular Structure Center. Because of possible variations in temperature and product composition, all analyses were carried out on single electron image plates. A new intermediate (15-cm) camera distance was utilized. General procedures for processing,<sup>7</sup> microphotometry,<sup>8</sup> and analyzing<sup>9</sup> the resultant data have been previously outlined. The procedures were modified, however, to handle multicomponent mixtures. In addition, mean-square amplitudes of vibration were not varied; they were either calculated or measured independently.

Numerous preliminary experiments failed to yield any evidence of the presence of DMSE. The nozzle was redesigned to achieve higher temperatures, and four promising plates were obtained (Table I). Plates I and II were recorded with a 20-ga (0.058-cm-i.d.) stainless steel nozzle and plates III and IV with a 16-ga (0.12-cm-i.d.) nozzle.<sup>10</sup> Analysis of each plate commenced with the construction of a radial distribution curve using the starting material, DMSCB, as a theoretical model. The extent and nature of decomposition could be assessed in this fashion. Difference curves (experimental—DMSCB) for plates I-IV are shown in Figure 1. The negative deviations at 1.56 Å corresponded to the carbon-carbon bond in DMSCB



**Figure 1.** Theoretical radial distribution curve for DMSCB and difference curves for plates I-IV.

**Table II.** Structural Parameters<sup>a</sup> for DMSE and Ethylene

plate	$r(\text{Si}=\text{C})$ , Å	$r(\text{Si}-\text{C})$ , Å	$r(\text{C}=\text{C})$ , Å
I	1.832 (64)	1.903 (35)	1.329 (200)
II	1.815 (36)	1.908 (17)	1.342 (54)
III	1.835 (41)	1.906 (20)	1.336 (82)
IV	1.832 (5)	1.905 (3)	1.346 (18)

<sup>a</sup> All distances  $r_g$  representations. Error limits in parentheses are three times the standard deviations.

and signaled the decomposition of DMSCB. The positive peaks at 1.34 Å indicated the formation of ethylene. Of greatest interest were the positive differences at 1.8 Å. This feature had not been observed in previous experiments and could reasonably be associated with the carbon-silicon double bond.<sup>3</sup> Moreover, the variation of these three difference peaks with changes in temperature and nozzle diameter (Table I) were consistent with the generation of DMSE and ethylene from DMSCB.

In the detailed analyses of plates I-IV, only four components were considered: DMSCB, DMSE, TMDSCB, and ethylene. Complementary vacuum line product studies supported this assumption and further indicated that ethylene and TMDSCB were stable under the reaction conditions. Electron diffraction data were collected for TMDSCB and ethylene under the same experimental conditions employed to pyrolyze DMSCB. Data were recorded for DMSCB slightly below the thermolysis threshold. High temperature structures for these three compounds were derived from the above data.<sup>10</sup> With the exception of the carbon-carbon bond length in ethylene, none of the structural parameters of DMSCB, TMDSCB, or ethylene were varied in the least-squares analyses of plates I-IV. The two carbon-silicon bond lengths of DMSE were varied, however, along with the mole fractions of the four components. All other DMSE parameters were assumed:  $r_g[(\text{C}-\text{H})\text{methyl}]$ ,<sup>11</sup> 1.11 Å;  $r_g[(\text{C}-\text{H})\text{methylene}]$ ,<sup>11</sup> 1.09 Å;  $\angle \text{C}=\text{SiC}$ ,<sup>3b,12</sup> 121°;  $\angle \text{HCSi}(\text{methyl})$ ,<sup>3b</sup> 110.8°;  $\angle \text{SiCH}(\text{methylene})$ ,<sup>3h</sup> 123°. The results of the least-squares analyses are reported in Tables I and II.<sup>10</sup>

A strict stoichiometric relationship between reactant and products was not observed (Table I). Considerable ethylene was lost between the pyrolysis zone and the electron beam. Fractionation of this sort is well known<sup>13</sup> and was verified in control experiments. The average carbon-carbon bond length of ethylene in plates I-IV was 1.34 Å (Table II) and provided an internal check on the usual calibration procedures.<sup>9a</sup> The average  $r_g(\text{C}=\text{Si})$  and  $r_g(\text{C}-\text{Si})$  values from Table II were  $1.83 \pm 0.04$  and  $1.91 \pm 0.02$  Å, respectively. The latter parameter is reasonable for a carbon-silicon single bond in this temperature range.<sup>14,15</sup> About a dozen quantum mechanical estimates of the carbon-silicon double bond length are available.<sup>3</sup> They vary from 1.63 to 1.75 Å. Most of the calculations are on CH<sub>2</sub>=SiH<sub>2</sub>. It is difficult to assess at this point how serious the discrepancy is between the measured and calculated bond lengths. For comparison purposes  $r_g(\text{C}=\text{Si})$  ought to be converted into a structural parameter more closely approximating an equilibrium ( $r_e$ ) bond length. Approximate calculations<sup>15</sup> indicate that this would only decrease the measured bond length by ~0.01-0.02 Å. A more important factor might

well be the influence of the methyl groups of DMSE. The only calculation that has been carried out on DMSE<sup>3b</sup> indicates that the methyl groups lengthen the carbon-silicon double bond by 0.04 Å.

Finally, it should be noted that the measured value of  $r_g(\text{C}=\text{Si})$  and the product distributions of Table I are in good agreement<sup>16</sup> with recent carbon-silicon  $\pi$ -bond energy measurements,<sup>17</sup> force fields derived from spectroscopic studies of matrix-isolated silaalkenes,<sup>4</sup> and the second-order rate constant for the dimerization of DMSE.<sup>18</sup>

**Supplementary Material Available:** Experimental conditions for plates I-IV; raw intensity data for DMSCB, TMDSCB, ethylene, and plates I-IV; theoretical models for DMSB, TMDSCB, and ethylene; error and correlation matrices; intensity curves and radial distribution curves for plates I-IV (23 pages). Ordering information is given on any current masthead page.

## References and Notes

- (a) L. E. Guse'nikov, N. S. Nametkin, and V. M. Vdovin, *Acc. Chem. Res.*, **8**, (1975); (b) M. Ishikawa, *Pure Appl. Chem.*, **50**, 11 (1978); (c) L. E. Guse'nikov and N. S. Nametkin, *Chem. Rev.*, **79**, 529 (1979).
- N. S. Nametkin, V. M. Vdovin, L. E. Guse'nikov, and V. I. Zav'yalov, *Izv. Akad. Nauk SSSR, Ser. Khim.*, 589 (1966).
- (a) R. Damrauer and D. R. Williams, *J. Organomet. Chem.*, **66**, 241 (1974); (b) M. J. S. Dewar, D. H. Lo, and C. A. Ramsden, *J. Am. Chem. Soc.*, **97**, 1311 (1975); (c) H. B. Schlegel, S. Wolfe, and K. Mislow, *J. Chem. Soc., Chem. Commun.*, 246 (1975); (d) P. H. Blustin, *J. Organomet. Chem.*, **105**, 161 (1976); (e) O. P. Strausz, L. Gammie, G. Theodorakopoulos, P. G. Mezey, and I. G. Csizmadia, *J. Am. Chem. Soc.*, **98**, 1622 (1976); (f) O. P. Strausz, M. A. Robb, G. Theodorakopoulos, P. G. Mezey, and I. G. Csizmadia, *Chem. Phys. Lett.*, **48**, 162 (1977); (g) R. Ahlrichs and R. Heinzmann, *J. Am. Chem. Soc.*, **99**, 7452 (1977); (h) D. M. Hood and H. F. Schaefer, III, *J. Chem. Phys.*, **68**, 2985 (1978); (i) J. C. Barthelat, G. Trinquier, and G. Bertrand, *J. Am. Chem. Soc.*, **101**, 3785 (1979).
- (a) O. L. Chapman, C. C. Chang, J. Koic, M. E. Jung, J. A. Lowe, T. J. Barton, and M. L. Tumej, *J. Am. Chem. Soc.*, **98**, 7845 (1976); (b) M. R. Chedekel, M. Skoglund, R. L. Kreeger, and H. Schechter, *ibid.*, **98**, 7846 (1976); (c) A. K. Mal'tsev, V. N. Khabashesky, and O. M. Nefodov, *Dokl. Akad. Nauk SSSR*, **223**, 421 (1977).
- A. G. Brook, S. C. Nyburg, W. F. Reynolds, Y. C. Poon, Y.-M. Chang, J.-S. Lee, and J.-P. Picard, *J. Am. Chem. Soc.*, **101**, 6750 (1979).
- P. G. Mahaffy, J. D. Wieser, and L. K. Montgomery, *J. Am. Chem. Soc.*, **99**, 4514 (1977).
- H. R. Foster, *J. Appl. Phys.*, **41**, 5344 (1970).
- H. R. Foster, D. A. Kohl, R. A. Bonham, and M. L. Williams, *Rev. Sci. Instrum.*, **43**, 605 (1972).
- (a) R. L. Hilderbrandt, J. D. Wieser, and L. K. Montgomery, *J. Am. Chem. Soc.*, **95**, 8598 (1973); (b) R. L. Hilderbrandt and J. D. Wieser, *J. Chem. Phys.*, **55**, 4648 (1971).
- Additional information is contained in the supplementary material.
- K. Kuchitsu, *MTP Int. Rev. Sci., Phys. Chem., Ser. One*, **11**, 221 (1972).
- Variation of the  $\angle\text{C}=\text{SiC}$  gave improved  $R$  factors. Because the least-squares values of the  $\angle\text{C}=\text{SiC}$  varied substantially from plate to plate, this parameter was constrained. Systematic studies indicated that this assumption did not significantly effect the carbon-silicon bond lengths.
- (a) E. W. Becker, K. Bier, and H. Burghoff, *Z. Naturforsch. A*, **10**, 565 (1955); (b) J. H. Chang, Ph.D. Thesis, Princeton University, 1967; (c) K. L. Gallaher and S. H. Bauer, *J. Phys. Chem.*, **78**, 2380 (1974).
- B. Beagley, J. J. Monaghan, and T. G. Hewitt, *J. Mol. Struct.*, **8**, 401 (1971).
- K. Kuchitsu and S. J. Cyvin in "Molecular Structures and Vibrations", S. J. Cyvin, Ed., Elsevier, New York, 1972, p 183.
- P. G. Mahaffy, Ph.D. Thesis, Indiana University, 1979.
- (a) L. E. Guse'nikov and N. S. Nametkin, *J. Organomet. Chem.*, **169**, 155 (1979); (b) W. J. Pietro, S. K. Pollack, and W. J. Hehre, *J. Am. Chem. Soc.*, **101**, 7126 (1979).
- L. E. Guse'nikov, K. S. Konobeevski, and V. M. Vdovin, *Dokl. Akad. Nauk SSSR*, **235**, 1086 (1977).

Peter G. Mahaffy, Robb Gutowsky  
Lawrence K. Montgomery\*

Department of Chemistry, Indiana University  
Bloomington, Indiana 47405

Received December 18, 1979

## Production of Dixenon Cation by Reversible Oxidation of Xenon<sup>1,2</sup>

Sir:

Dixenon cation,  $\text{Xe}_2^+$ , is a principal product of the reduction of xenon(II) in antimony pentafluoride solutions. The bright

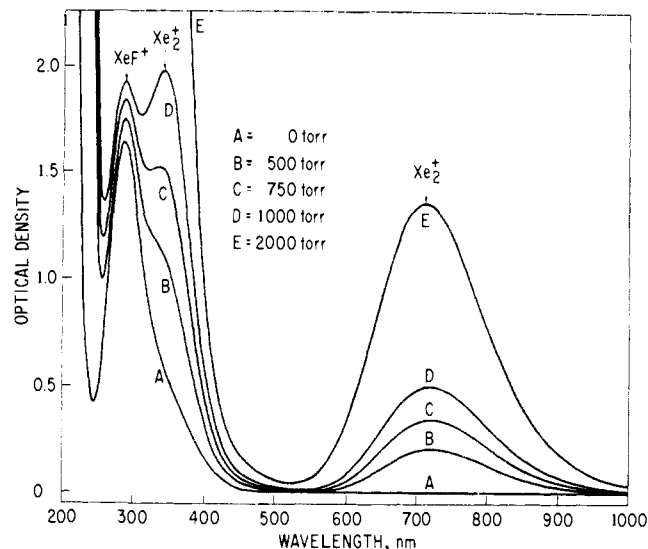
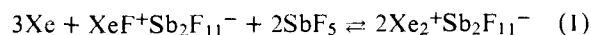


**Figure 1.** The effect of xenon pressure upon the UV-visible spectrum of a solution of  $\text{XeF}^+\text{Sb}_2\text{F}_{11}^-$  in antimony pentafluoride at 25 °C: curve A, 0.404 M  $\text{XeF}^+\text{Sb}_2\text{F}_{11}^-$  in the absence of xenon gas (yellow); curves B, C, D, and E, the same solution in equilibrium with xenon at partial pressures shown in the figure (green). The bands at 287 and 335 nm are off scale in curve E. The spectra were obtained with a Cary 14 spectrometer, using a 0.1-cm-path-length cell.

green, paramagnetic ion has been characterized by its Raman, UV-visible, and ESR spectra<sup>3</sup> and has been shown to be formed as an intermediate product in reactions of elemental xenon with dioxygenyl salts. We have found that the cation can also be produced by adding xenon gas to a solution of  $\text{XeF}^+\text{Sb}_2\text{F}_{11}^-$  in antimony pentafluoride and can be decomposed by pumping off the gas. At 20 °C, the solution frequently separates into two liquid phases, a pale green upper phase containing low concentrations of  $\text{Xe}_2^+$ ,  $\text{XeF}^+$ , and  $\text{Sb}_2\text{F}_{11}^-$  ions and a dark green bottom phase containing high concentrations of these ions. We report here the results of a preliminary study of this reaction—the first to produce a noble-gas species by reversible oxidation at ambient temperature.

A thoroughly degassed solution of  $\text{XeF}^+\text{Sb}_2\text{F}_{11}^-$  is pale yellow and exhibits only a single band of  $\text{XeF}^+$  cation at 287 nm in its UV-visible spectrum, as shown in curve A, Figure 1. When xenon gas is added to a pressure of 500 Torr and the solution is stirred until equilibrium is reached (~30 min), the solution turns green and a new spectrum is obtained (curve B). Bands of  $\text{Xe}_2^+$  cation then become visible at 335 and 720 nm.<sup>4</sup> As the xenon pressure is increased, these bands increase in intensity but very little change occurs in the band at 287 nm. (The apparent increase in height of this band is due to overlap with the adjacent  $\text{Xe}_2^+$  band.) Upon removal of the xenon, the bands of  $\text{Xe}_2^+$  disappear and the spectrum reverts to its original shape. The Raman band of  $\text{Xe}_2^+$  at 123  $\text{cm}^{-1}$  and the ESR signal of  $\text{Xe}_2^+$  also appear and disappear in corresponding fashion in Raman and ESR spectra, respectively. We have found that this process can be repeated many times and is highly reproducible. A reversible reaction therefore occurs in this system between xenon and  $\text{XeF}^+\text{Sb}_2\text{F}_{11}^-$ .

The dependence of the optical density of the band at 720 nm upon xenon pressure and upon the concentration of  $\text{XeF}^+\text{Sb}_2\text{F}_{11}^-$  does not correspond to that which would be expected for the simplest possible equilibrium



This requires that the concentration of  $\text{Xe}_2^+$  be proportional to the  $3/2$  power of the xenon pressure (inasmuch as Henry's Law is obeyed by xenon in antimony pentafluoride), the square root of the  $\text{XeF}^+\text{Sb}_2\text{F}_{11}^-$  concentration, and the first power of the antimony pentafluoride concentration. Instead, we find